

On the Formation of a Macroscopically Flat Phospholipid Membrane on a Hydrosol Substrate

A. M. Tikhonov^a, V. E. Asadchikov^b, and Yu. O. Volkov^b

^a Kapitza Institute for Physical Problems, Russian Academy of Sciences, ul. Kosygina 2, Moscow, 119334 Russia

^b Shubnikov Institute of Crystallography, Russian Academy of Sciences, Leninskii pr. 59, Moscow, 119333 Russia

e-mail: tikhonov@kapitza.ras.ru

Received August 3, 2015

The dependence of the structure of a phospholipid layer (DSPC and SOPC) adsorbed on a hydrosol substrate on the concentration of NaOH in a solution of 5-nm silica particles has been studied by X-ray reflectometry with the use of synchrotron radiation. Profiles of the electron density (polarizability) have been reconstructed from the experimental data within a model-independent approach. According to these profiles, the thickness of the lipid film can vary from a monolayer (~ 35 Å) to several bilayers (~ 450 Å). At the volume concentration of NaOH of ~ 0.5 mol/L, the film on the hydrosol surface is a macroscopically flat phospholipid membrane (bilayer) with a thickness of ~ 60 Å and with areas of (45 ± 2) and (49 ± 3) Å² per DSPC and SOPC molecule, respectively.

DOI: 10.1134/S0021364015190157

A phospholipid bilayer is the simplest model of a cell membrane [1–3]. The method of obtaining macroscopically flat multilayers of lipid membranes on a strongly polarized substrate of an aqueous solution of amorphous silica nanoparticles was proposed in our work [4]. Using a model-independent approach to reconstruct electron density profiles [5, 6], we revealed from the X-ray reflectometry data that the thickness of a phospholipid multilayer is determined by the following parameters of the hydrosol substrate, which specify the width of the surface electric double layer: the concentration of Na⁺, pH level, and size of nanoparticles. In particular, a macroscopically flat phospholipid membrane spontaneously appears on the surface of the hydrosol of 5-nm particles under certain conditions.

Films of 1,2-distearoyl-sn-glycero-3-phosphocholine (DSPC) and 1-stearoyl-2-oleoyl-sn-glycero-3-phosphocholine (SOPC, see Fig. 1) were prepared and studied with the methodology described in [4]. A 10- to 20- μ L drop of a solution of phospholipid in chloroform was deposited from a syringe on the surface of the liquid substrate placed on a fluoroplastic plate with a diameter of ~ 100 mm; the amount of substance in the drop was enough for the formation of more than ten lipid monolayers after its spreading on the surface. In this case, the adsorbed film is in equilibrium with three-dimensional aggregates in which an excess of the surfactant is accumulated. A change in the surface tension γ of the air–hydrosol interface from ~ 74 to ~ 50 – 30 mN/m was detected by the Wil-

helmy method using an NIMA PS-2 surface pressure sensor. Then, the equilibrium of the sample was reached inside a hermetic single-stage thermostat at $T = 298$ K in about 12 h.

Powders of synthetic DSPC and SOPC and their solutions in chloroform was purchased from Avanti Polar Lipids and chloroform ($\sim 99.8\%$) was purchased from Sigma-Aldrich. The hydrophobic part of molecules of these lipids ($L_1 \approx 2$ nm) consists of two hydrocarbon chains including 18 carbon atoms. The hydrophilic part of the molecule ($L_2 \approx 1.5$ nm) is formed by glycerin and phosphocholine. The only difference between the structures of DSPC and SOPC is the presence of a double carbon bond between the ninth and tenth atoms in one of the hydrocarbon chains in the latter molecule. The DSPC (or C₄₄H₈₈NO₈P) and SOPC (or C₄₄H₈₆NO₈P) molecules contain $\Gamma = 438$ and 436 electrons, respectively.

Concentrated monodisperse Ludox FM sol stabilized by sodium hydroxide was obtained from the Grace Davison Co. This aqueous solution with a den-

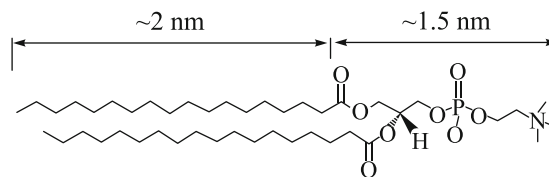


Fig. 1. Molecular structure of the DSPC phospholipid.

sity of 1.1 g/cm^3 includes amorphous silica particles with the diameter $D \approx 5 \text{ nm}$ (16 wt % SiO_2 , 0.3 wt % Na, and $\text{pH} \approx 10$).

The NaOH hydrosol was enriched in a vessel by its mixing (shaking and subsequent deposition in a Branson 2510 ultrasonic cleaner) with a solution ($\sim 5 \text{ mol/L}$) of alkali metal oxide (99.95% of the metal, Sigma-Aldrich) in deionized water (Barnstead UV). It is very important that the pH level of sol not exceed the critical value $\text{pH}_c < 12$, at which coagulation of nanoparticles occurs [7].

The surface-normal structure of lipid films was studied by the reflectometry method with the use of synchrotron radiation at the X19C station of the NSLS synchrotron, which was equipped with a universal spectrometer for study of the surface of a liquid [8]. A bending magnet with a critical energy of $\sim 6 \text{ keV}$ was used as a source of radiation for the X19C station. A focused monochromatic X-ray beam with an intensity of $\approx 10^{11}$ photon/s and an energy of photons $E = 15 \text{ keV}$ ($\lambda = (0.825 \pm 0.002) \text{ \AA}$) was used in the experiments. The beam whose cross section at the output of the magnet had a height of 5 mm and a width of 40 mm was focused by a toroidal mirror with a focal length of $\sim 10 \text{ m}$. Then, the beam with the diameter of the cross section less than 1 mm was deflected by means of a single-crystal (Si (111)) monochromator to the surface of the sample oriented by the gravitational force. Thus, the range of the glancing angle α from 0° to $\sim 8^\circ$ could be covered when measuring the reflection coefficient. The monochromator of the spectrometer was based on a three-circle goniometer (Huber), had water cooling, and was placed in a hermetic chamber filled with gaseous helium at a low excess pressure ($\sim 10 \text{ Torr}$). The geometric parameters of the beam incident on the surface of the sample, as well as the spatial resolution of the detector, were controlled in the experiments by means of slits. In this work, the reflection coefficient was measured by a detector with the angular resolutions $\Delta\beta \approx 0.02^\circ$ and 0.8° in the vertical and horizontal planes, respectively.

Let \mathbf{k}_{in} and \mathbf{k}_{sc} be the wave vectors of the incident beam and the beam scattered in the direction to the observation point, respectively. The scattering vector $\mathbf{q} = \mathbf{k}_{\text{in}} - \mathbf{k}_{\text{sc}}$ at mirror reflection ($\alpha = \beta$) has only one component $q_z = (4\pi/\lambda)\sin\alpha$, where α and β are the glancing and scattering angles, respectively, in the plane normal to the surface (see inset in Fig. 2).

When measuring the reflection curve, the effect of lateral inhomogeneities of the surface and near-surface layers is averaged because the characteristic area of the region illuminated by a probe beam on the sample is $\sim 100 \text{ mm}^2$. As a result, the reconstructed structures can be considered within the notion of an ideal layered inhomogeneous medium.

The detailed reconstruction of the distributions of the polarizability of the medium $\delta(z)$ over the depth z

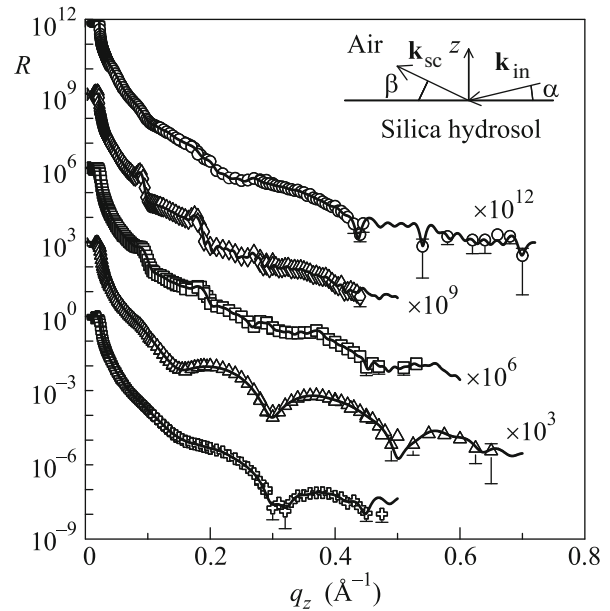


Fig. 2. Reflection coefficient R of the air–hydrosol interface with the adsorbed lipid film for (circles) the DSPC monolayer ($\text{pH} \approx 10$); (diamonds) the DSPC multilayer ($\text{pH} \approx 10$); (squares) the DSPC multilayer ($\text{pH} \approx 11$); (triangles and crosses) the DSPC and SOPC bilayers, respectively ($\text{pH} \approx 11.5$); and (solid lines) calculations. The inset shows the wave vectors \mathbf{k}_{in} and \mathbf{k}_{sc} of the incident beam and the beam scattered in the direction to the observation point, respectively.

was performed within a model-independent approach based on the extrapolation of the asymptotic angular dependence of the reflection coefficient to the region of large α values [5, 6]. It is assumed that the reconstructed structure includes peculiar “points of discontinuity” at which either $\delta(z)$ or its n th derivative $\delta^{(n)}(z)$ changes stepwise:

$$\mathbf{D}^{(n)}(z_j) \equiv \frac{d^n \delta}{dz^n}(z_j + 0) - \frac{d^n \delta}{dz^n}(z_j - 0), \quad (1)$$

where z_j is the coordinate of the j th point of discontinuity. In turn, the asymptotic behavior of the amplitude reflection coefficient in the first Born approximation has the form

$$r(q_z \rightarrow \infty) \approx -\left(\frac{2\pi}{\lambda}\right)^2 \left(\frac{i}{q_z}\right)^{n+2} \sum_{j=1}^m \mathbf{D}^{(n)}(z_j) e^{iq_z z_j}. \quad (2)$$

According to [5], a finite number of different amplitude reflection coefficients describing the experimentally measured square of their absolute value R in a certain interval of q_z correspond to a given combination of m points of discontinuity of $\mathbf{D}^{(n)}(z)$. In particular, if the distances between all points of discontinuity are different, there are only two solutions $\delta(z)$ satisfying the required asymptotic behavior of the reflection curve.

The procedure of the model-independent reconstruction of the polarizability profile includes two stages. First, the order and positions of the points of discontinuity for the structure under study are determined by analyzing the dependence Rq_z^{2n+4} (where $n = 0, 1, 2, \dots$ is the desired order of singular points). Then, the distribution $\delta(z_1, \dots, z_M)$ divided into a large number $M \sim 100$ of thin layers is numerically optimized. In this case, the calculated reflection curve R_c is fitted to the experimentally measured curve R with the use of the standard Levenberg–Marquardt algorithm [9].

All experimental curves in this work decrease as $1/q_z^6$. Consequently, to describe the structures, it is sufficient to use only the singular points of the first order. In this case, the residual target function ensuring the required asymptotic behavior of the angular dependence of the reflection coefficient has the form

$$\begin{aligned} & MF(\delta_1, \dots, \delta_M) \\ &= \frac{1}{N} \sum_{j=1}^N [\log R(q_j) - \log R_c(q_j)]^2 \\ &+ Q_1 \sum_{\substack{j=1, \dots, M-1 \\ j \neq j_1, \dots, j_m}} (\delta_{j-1} + \delta_{j+1} - 2\delta_j)^2 \\ &+ Q_2 \sum_{j=j_1, \dots, j_m}^m (\delta_{j+1} - \delta_j), \end{aligned} \quad (3)$$

where N is the number of experimental points; j_1, \dots, j_m are the positions of the points of discontinuity; and $Q_{1,2} \approx 10^9$ are the parameters controlling the accuracy of fitting. The second sum in Eq. (3) ensures the continuity of the profile $\delta(z)$ in the intervals between the points of discontinuity z_1, \dots, z_m , and the third sum ensures the first order of points of discontinuity.

The reconstructed profile $\delta(z)$ corresponds to the electron density distribution $\rho(z)$ [10]:

$$\rho = \frac{2\pi}{r_0 \lambda^2} \delta, \quad (4)$$

where $r_0 = 2.814 \times 10^{-5} \text{ \AA}$ is the classical radius of the electron. Then, the dependence $\rho(z)$ can be used, e.g., to estimate the area A per molecule in a monolayer with the thickness $d = z_2 - z_1$:

$$A = \frac{\Gamma}{z_2} \int_{z_1} \rho(z) dz \quad (5)$$

Figure 2 shows the experimental dependences of the reflection coefficient $R(q_z)$ for the interfaces between air and the hydrosol of 5-nm particles with the adsorbed lipid film. Circles correspond to the surface of the sol with $\text{pH} \approx 10$ (Ludox FM) where the amount of deposited DSPC is insufficient for the formation of a uniform monolayer on the entire surface of

the substrate. The period of oscillation of R for this system is $\Delta q_z \approx 0.25 \text{ \AA}^{-1}$, which implies the presence of an adsorbed monolayer ($\sim 2\pi/\Delta q_z \approx 30 \text{ \AA}$) in the illumination region. Diamonds show the dependence $R(q_z)$ for the same surface of the sol with $\text{pH} \approx 10$ but with a homogeneous DSPC multilayer. Squares correspond to the surface of the NaOH-enriched ($\sim 0.3 \text{ mol/L}$) sol with $\text{pH} \approx 11$ with the same phospholipid multilayer. The last two dependences are similar to the previously reported data for hydrosol substrate with silica particles with a diameter of $\sim 22 \text{ nm}$ and $\text{pH} \approx 9$ [4]. The data presented by triangles (DSPC layer) and crosses (SOPC layer) were obtained for NaOH-enriched ($\sim 0.5 \text{ mol/L}$) substrates with $\text{pH} \approx 11.5$. The period of oscillations R for these data is $\Delta q_z \approx 0.15 \text{ \AA}^{-1}$; i.e., the thickness of the adsorbed layer $\sim 2\pi/\Delta q_z \approx 50 \text{ \AA}$ (bilayer).

According to the $\rho(z)$ profile reconstructed for the DSPC monolayer (Fig. 3a, where $\rho_w = 0.333 \text{ e}^-/\text{\AA}^3$ is the electron density in water under normal conditions), its thickness is $(36 \pm 2) \text{ \AA} \approx L_1 + L_2$; i.e., all molecules are predominantly oriented along the normal to the surface. Although the calculated area per molecule $A = (44 \pm 2) \text{ \AA}^2$ is in good agreement with the value for the crystal monolayer, the electron density in the region of the hydrophilic group is lower than

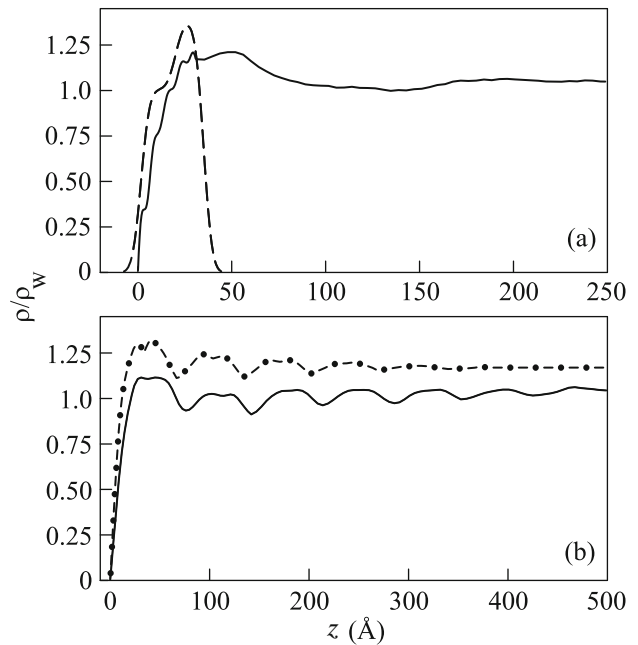


Fig. 3. Reconstructed distribution profiles $\rho(z)$ normalized to the electron density in water under normal conditions, $\rho_w = 0.333 \text{ e}^-/\text{\AA}^3$. (a) The solid line is for the DSPC monolayer on the surface of the hydrosol of ~ 5 -nm particles and the dashed line is the model electron density distribution for the DSPC monolayer [4]. (b) The solid line is for the DSPC multilayer on the hydrosol substrate with $\text{pH} \approx 10$ and dash-dotted line is for the same lipid multilayer on the substrate with $\text{pH} \approx 11$.

that in the model distribution (dashed line in Fig. 3a) for the DSPC monolayer from [4]. This likely indicates the incomplete filling of the lipid layer.

The layer with an increased density $\rho \approx 1.2\rho_w$ with the thickness ≈ 50 Å directly follows the monolayer and the next layer has a thickness of ~ 80 Å and an electron density of $\approx \rho_w$. We attribute the formation of the last two layers to the condensation of silica nanoparticles at the boundary of the monolayer formed by hydrophilic groups [11].

The profile of the DSPC multilayer on the surface of the hydrosol with $\text{pH} \approx 10$ (solid line in Fig. 3b) has a six-layer structure (total thickness ~ 450 Å) with the period between the points of discontinuity of (72 ± 2) Å, which corresponds to the doubled length of the DSPC molecule. Assuming that each of the observed layers is equivalent to a molecular bilayer, we calculated the value $A = (39 \pm 1)$ Å². At the same time, according to the experimental data on grazing diffraction, $A = (41.6 \pm 0.7)$ Å² [4]. Thus, according to Eq. (5), the excess number of electrons per lipid molecule is 32 ± 9 , which corresponds to about three H₂O molecules and/or Na⁺ ions. The thickness of the DSPC multilayer on the substrate with $\text{pH} \approx 11$ is noticeably smaller (~ 300 Å, the dash-dotted line in Fig. 3b). This multilayer has a four-layer structure with the period between the points of discontinuity of (68.1 ± 0.9) Å and with the calculated value $A = (34 \pm 2)$ Å². Thus, the “excess” number of electrons per lipid molecule is 86 ± 2 , which corresponds to ~ 9 H₂O molecules and/or Na⁺ ions.

Figure 4a shows the electron density profile for a thin film of the DSPC lipid on hydrosol heavily enriched in NaOH (~ 0.5 mol/L, $\text{pH} \approx 11.5$). One of the points of discontinuity in it is located at a depth of 30.6 Å. Assuming that the position of this singular point corresponds to the interface between the outer and inner monolayers, we obtain $A = (45 \pm 2)$ Å².

The denser layer adjacent to this interface has a thickness of ~ 20 Å. On one hand, its thickness is slightly smaller than that of the DSPC monolayer and the total density is close to the total density of the latter monolayer. On the other hand, the thickness of this layer is less than half of the characteristic diameter of particles in the volume of the initial sol (≈ 5 nm). If this layer is formed by colloid particles, it is necessary to assume that their radius decreases significantly with an increase in the concentration of sodium in a solution. However, at a high concentration of Na⁺, an inverse process—coagulation of particles, which is manifested, e.g., in the turbidity of the solution—was experimentally observed [7]. This allows the interpretation of this distribution as a profile of the lipid bilayer on the surface of the hydrosol.

For the SOPC lipid film on the substrate with $\text{pH} \approx 11.5$, the thickness of the dense region is no more than 60 Å (Fig. 4b). In this case, $\rho(z)$ decreases

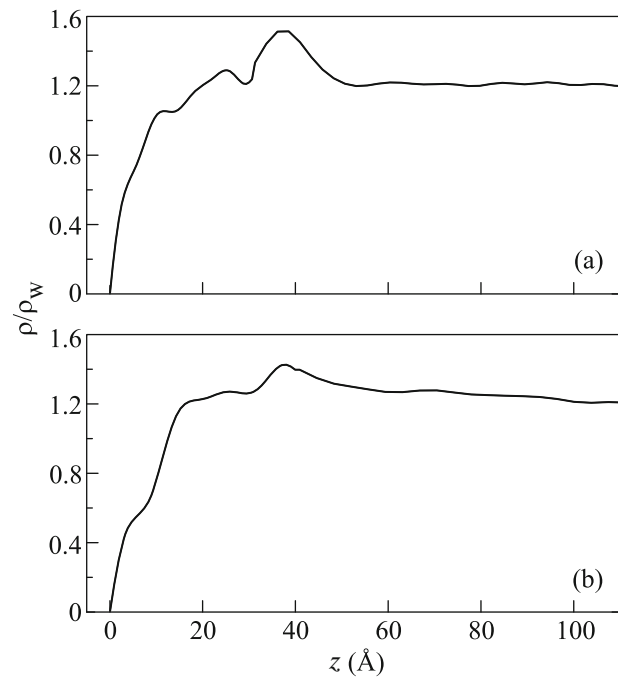


Fig. 4. Reconstructed distribution profiles $\rho(z)$ normalized to the electron density in water under normal conditions, $\rho_w = 0.333 \text{ e}^-/\text{Å}^3$, for the (a) DSPC and (b) SOPC membranes on the substrate with $\text{pH} \approx 11.5$.

smoothly with the depth and, correspondingly, no interface between the film and substrate is observed. No pronounced stratification of silica nanoparticles in the surface region is observed either. The total density of the entire observed structure at depths up to 57 Å is more than twice as large as the theoretical value for the monolayer of this lipid. Under the assumption that the amount of SOPC in the film corresponds to two (three) monolayers, we obtain $A = (49 \pm 3)$ Å² ((65 ± 3) Å²). Only the latter value is in agreement with the estimate of the quantity A for bilayer walls of SOPC vesicles in aqueous suspensions [12].

Electron density profiles for the DSPC and SOPC films in Fig. 4 have a very similar structure. At the same time, DSPC and SOPC phospholipids have different temperatures T_c of a phase transition associated with the melting of hydrocarbon chains (chain-melting transition) [2]. For the former phospholipid, $T_c \approx 55^\circ\text{C}$, which explains the formation of the macroscopically flat crystalline membrane ($A = (45 \pm 2)$ Å²). For SOPC, $T_c \approx 6^\circ\text{C}$ and the parameter A is $\sim 10\%$ larger than that for DSPC. Thus, the SOPC membrane at room temperature is possibly in a liquid aggregate state.

For the last two systems, the interval z in which the surface electron density differs from the bulk density, $\rho_b \approx 1.2\rho_w$, is 50–60 Å wider than the thickness of the bilayer (~ 60 Å). The appearance of this transient

Parameters of structures on the surface of the NaOH-stabilized sol of 5-nm SiO₂ particles: the thickness L and the surface area A per lipid molecule

Structure	Phospholipid	pH	L , Å	A , Å ²
Monolayer	DSPC	10	36 ± 2	44 ± 2
Bilayer in a multilayer	DSPC	10	72 ± 2	41.6 ± 0.7
Bilayer in a multilayer	DSPC	11	68 ± 1	41.6 ± 0.7
Bilayer	DSPC	11.5	60 ± 2	45 ± 2
Bilayer	SOPC	11.5	60 ± 2	49 ± 3

region is possibly due to the condensation of silica nanoparticles at the edge of the lipid membrane [11].

It was previously shown that a very wide transient layer (electric double layer) appearing because of the difference between the potentials of the forces of the electric image for Na⁺ cations and negatively charged silica nanoparticles (macroions) exists at the (air–silica sol) interface [13]. Its width is determined by the Debye screening length Λ_D in the bulk of the solution [1]. The addition of sodium hydroxide to the composition of the sol results in the shift of chemical equilibrium in it, which is accompanied by an increase in the pH value of the solution or the volume concentration c^- of OH⁻ ions. Since $\Lambda_D \propto 1/\sqrt{c^-}$, an increase in pH leads to the narrowing of the double surface layer [14].

The set of our data indicates that the total thickness of the adsorbed DSPC multilayer is $\sim \Lambda_D$ (see table). The enrichment of the hydrosol substrate with NaOH results in a decrease by several times in the maximum thickness of the adsorbed lipid layer according to a decrease in Λ_D . The thickest (~ 450 Å) multilayer of six DSPC bilayers is formed on the surface of the hydrosol at pH ≈ 10 ($\Lambda_D \sim 300$ Å), the multilayer with a thickness of ~ 300 Å at pH ≈ 11 ($\Lambda_D \sim 100$ Å) consists of four bilayers, and one bilayer appears at pH ≈ 11.5 ($\Lambda_D \sim 50$ Å). In this case, the oriented packing of molecules inside each bilayer corresponds to a two-dimensional phospholipid crystal.

To summarize, electron density profiles reconstructed within the model-independent approach demonstrate that the thickness of the DSPC film adsorbed on the surface of the hydrosol coincides in order of magnitude with the Debye screening length in the substrate. At the volume concentration of NaOH ~ 0.5 mol/L and pH ≈ 11.5 , a macroscopically flat phospholipid membrane with a thickness of ~ 60 Å and with the A value characteristic of a two-dimensional crystal (hexagonal phase P_β , [2, 4]) is formed on the surface of the hydrosol. The A value for SOPC is at least $\sim 10\%$ larger than that for the DSPC bilayer. In this case, the formation of a liquid membrane with a thickness of ~ 60 Å (phase L_α [2]) is possible.

The work at the NSLS synchrotron was supported by the US Department of Energy (contract no. DE-AC02-98CH10886). The work at the X19C station was supported by the ChemMatCARS Foundation, University of Chicago, University of Illinois at Chicago, and Stony Brook University. We are grateful to the Grace Davison Co. for the Ludox silica colloidal solution. This work was supported in part by the Russian Foundation for Basic Research (project no. 15-32-20935).

REFERENCES

1. A. W. Adamson, *Physical Chemistry of Surfaces*, 3rd ed. (Wiley, New York, 1976).
2. D. M. Small, *The Physical Chemistry of Lipids* (Plenum, New York, 1986).
3. D. A. Los', *Fatty Acids Desaturases* (Nauchn. Mir, Moscow, 2014) [in Russian].
4. A. M. Tikhonov, *JETP Lett.* **92**, 356 (2010).
5. I. V. Kozhevnikov, *Nucl. Instrum. Methods Phys. Res. A* **508**, 519 (2003).
6. I. V. Kozhevnikov, L. Peverini, and E. Ziegler, *Phys. Rev. B* **85**, 125439 (2012).
7. J. Depasse and A. Watillon, *J. Coll. Int. Sci.* **33**, 430 (1970).
8. M. L. Schlossman, D. Synal, Y. Guan, M. Meron, G. Shea-McCarthy, Z. Huang, A. Acero, S. M. Williams, S. A. Rice, and P. J. Viccaro, *Rev. Sci. Instrum.* **68**, 4372 (1997).
9. J. Nocedal and S. Wright, *Numerical Optimization*, 2nd ed. (Springer, Berlin, 2006).
10. B. L. Henke, E. M. Gullikson, and J. C. Davis, *Atom. Data Nucl. Data Tables* **54**, 181 (1993).
11. V. E. Asadchikov, V. V. Volkov, Yu. O. Volkov, K. A. Dembo, I. V. Kozhevnikov, B. S. Roshchin, D. A. Frolov, and A. M. Tikhonov, *JETP Lett.* **94**, 585 (2011).
12. N. Kučerka, M.-P. Mieh, and J. Katsaras, *Biochem. Biophys. Acta* **1808**, 2761 (2011).
13. A. M. Tikhonov, *J. Phys. Chem. C* **111**, 930 (2007).
14. A. M. Tikhonov, *J. Chem. Phys.* **124**, 164704 (2006).

Translated by R. Tyapayev